DISSIPATION DYNAMICS OF NUCLEAR FUSION REACTIONS*

Kai Wen, M.C. Barton, A. Rios, P.D. Stevenson

Faculty of Engineering and Physical Sciences, University of Surrey
Guildford, Surrey, GU2 7XH, United Kingdom

(Received November 16, 2018)

Based on both the time-dependent Hartree–Fock (TDHF) and the time-dependent density matrix (TDDM) methods, we adopt a macroscopic reduction procedure to investigate the dissipation dynamics of nuclear fusion reactions. The TDDM method is an extension of TDHF, in the sense that it goes beyond the mean-field concept and takes into account two-body correlations explicitly. To investigate the effect of correlations on dissipation, the collective trajectories as well as the friction coefficients for the reaction $^{16}\mathrm{O} + ^{16}\mathrm{O} \rightarrow ^{32}\mathrm{S}$ are extracted. Our results suggest that two-body correlations play a relevant role in the fusion process.

DOI:10.5506/APhysPolB.50.567

1. Introduction

As a non-equilibrium process involving many-body dynamics, the microscopic mechanism at the heart of dissipation in nuclear fusion reactions has been a baffling subject for decades. At a theoretical level, this mechanism can be understood by implementing numerical simulations with a microscopic theoretical basis. Based on the mean-field concept, the time-dependent Hartree–Fock (TDHF) model is recognised as a generic theoretical framework to simulate low-energy nuclear dynamics. TDHF has been extensively applied to study nuclear reactions [1], and there have been several significant developments in real time dynamical simulations in the recent past [2–5]. TDHF, however, has limitations. On the one hand, genuine two-body correlations are neglected at the microscopic level. On the other hand, despite the quantum mechanical property embodied at single-particle level, TDHF has a semi-classical nature at the collective level.

* Presented at the Zakopane Conference on Nuclear Physics "Extremes of the Nuclear Landscape", Zakopane, Poland, August 26–September 2, 2018.

In theory, the exact solution of the many-body dynamics is given by equations that go beyond the mean-field approach. When projected into density matrices, those equations can be expressed in terms of the Bogoliubov–Born–Green–Kirkwood–Yvon (BBGKY) hierarchy [6]. TDHF arises as the lowest order truncation in the BBGKY hierarchy, which assumes that two- and higher-body correlations are negligible. To go beyond TDHF and account for dynamical effects on the two-body density matrix, the following order in the scheme needs to be implemented [7–10]. This so-called Time-Dependent Density Matrix (TDDM) approach extends the TDHF method by including genuine two-body correlations that can modify the structure of the one-particle density matrix.

The numerical cost associated with the solution of the corresponding coupled equations is however very high. A technique that can significantly reduce the numerical cost is to simulate the dynamics in a moving basis that is the solution of a TDHF-like equation [7, 9]. Further, if one only considers the beyond mean-field interaction between time-reversed pairs, a more applicable version of TDDM arises. This is the so-called TDDM$^{\mathrm{P}}$ scheme [11] which has been successfully applied to study the effect of nuclear correlations on the breakup mechanism [11]. In this work, we carry out numerical simulations using both TDHF and TDDM$^{\mathrm{P}}$.

The paper is organized as follows. In Sec. 2, we introduce the theoretical framework and numerical simulations. These are applied to study dissipative processes in the fusion reaction $^{16}\mathrm{O} + ^{16}\mathrm{O} \leftrightarrow ^{32}\mathrm{S}$ in Sec. 3. A summary and concluding remarks are given in Sec. 4.

2. Theoretical framework

The BBGKY hierarchy that governs the exact solution of many-body density matrices reads

$$
\begin{aligned}
i\frac{\partial}{\partial t}\rho^{(1)}(t) &= \left[t_1, \rho^{(1)}(t)\right] + \mathrm{tr}_{(2)}\left[v_{12}, \rho^{(2)}(t)\right] , \\
i\frac{\partial}{\partial t}\rho^{(2)}(t) &= \left[t_1 + t_2 + v_{12}, \rho^{(2)}(t)\right] + \mathrm{tr}_{(3)}\left[v_{13} + v_{23}, \rho^{(3)}(t)\right] , \\
&\vdots \\
i\frac{\partial}{\partial t}\rho^{(n-1)}(t) &= \left[\sum_{i=1}^{n-1} t_i + \sum_{i,j=1}^{n-1} v_{ij}, \rho^{(n-1)}(t)\right] + \sum_{i=1}^{n-1} \mathrm{tr}_{(n)}\left[v_{i,k+1}, \rho^{(n)}(t)\right] ,
\end{aligned}
$$

where $\rho^{(n)}$ represents the n-body density matrix and, therefore, depends on $2 \times n$ spatial, spin and isospin variables. v is the two-body interaction and t_i is the kinetic energy operator of the i^{th} particle. The traces $\mathrm{tr}_{(n)}$ are taken over the degrees of freedom of particle n.

For the A-body problem, the hierarchy would consist of $A-1$ coupled differential equations. The TDDM method aims to solve the time evolution of both $\rho^{(1)}$ and $\rho^{(2)}$, assuming three-body and higher-order correlations are negligible. For convenience, we use the two-body correlation matrix $C^{(2)}$, which is customarily defined as the correlated part of the two-body density matrix, $C^{(2)} = \rho^{(2)} - \hat{A}(\rho^{(1)}\rho^{(1)})$, where $\hat{A}$ stands for an antisymmetrization operator. As mentioned in the last section, to make the problem numerically feasible, $\rho^{(1)}$ and $C^{(2)}$ are expanded in a moving basis set with a finite number of single-particle states. These evolve in time obeying a TDHF-like equation of motion

$$i\hbar\dot{\psi}_i(\boldsymbol{r},t) = \hat{h}\left(t,\rho^{(1)}\right)\psi_i(\boldsymbol{r},t)\,, \qquad i = 1\ldots N_{\max}\,. \tag{1}$$

We note that the mean-field Hamiltonian, $\hat{h}\left(t,\rho^{(1)}\right)$, depends on the correlated rather than the mean-field, one-body density matrix.

In the TDDM^P method, the equations that determine the dynamics of $\rho^{(1)}$ and $C^{(2)}$ read

$$\dot{\rho}^{(1)}_{\alpha} = \frac{2}{\hbar}\sum_{\gamma}\mathrm{Im}\left(V_{\alpha\gamma}C^{(2)}_{\gamma\alpha}\right)\,, \tag{2}$$

$$\begin{aligned} i\hbar\dot{C}^{(2)}_{\alpha\beta} &= V_{\alpha\beta}\left[\left(1-\rho^{(1)}_{\alpha}\right)^2\left(\rho^{(1)}_{\beta}\right)^2 - \left(1-\rho^{(1)}_{\beta}\right)^2\left(\rho^{(1)}_{\alpha}\right)^2\right] \\ &\quad + \sum_{\gamma}V_{\alpha\gamma}\left(1-2\rho^{(1)}_{\alpha}\right)C^{(2)}_{\gamma\beta} - \sum_{\gamma}V_{\gamma\beta}\left(1-2\rho^{(1)}_{\beta}\right)C^{(2)}_{\alpha\gamma}\,. \end{aligned} \tag{3}$$

Here, the Greek indexes $\alpha,\beta,\ldots$ represent a pair of time reversed states — *e.g.* α and its time conjugate partner, $\bar{\alpha}$. $V_{\alpha\beta}$ is the antisymmetric interaction matrix element, $V_{\alpha\beta} = \langle\alpha\bar{\alpha}|v|\beta\bar{\beta}\rangle_A$, and $C^{(2)}_{\alpha\beta}$ is the corresponding correlation tensor matrix element, $C^{(2)}_{\alpha\beta} = \langle\alpha\bar{\alpha}|C^{(2)}|\beta\bar{\beta}\rangle$.

In practical calculations, a finite basis evolving with Eq. (1) spoils the energy conservation of the TDDM model [7]. Since energy conservation is of paramount importance in the discussion of dissipative dynamics, we have devised a technique to enforce energy conservation by optimizing the moving basis [12]. This is implemented in the results discussed hereafter.

3. Numerical results

3.1. Correlated ground state

We take advantage of the adiabatic switching technique [13] to obtain the correlated ground state from the Hartree–Fock (HF) static state. We switch on adiabatically the residual interaction, which takes the form of

$$v_{12}\left(\vec{r}_1,\vec{r}_2,t\right)=\left(1-e^{-\frac{t^2}{\tau^2}}\right)V_0\left[1-\frac{\rho}{\rho_0}\right]\delta^{(3)}\left(\vec{r}_1-\vec{r}_2\right)\,. \tag{4}$$

This residual interaction is the standard choice in the literature [10], but differs from the mean-field interaction which in this work is the Skyrme III [14] parametrization of the Skyrme interaction. We use a model space of $N_{\max}=30$ orbits for ^{16}O. Figure 1 shows the evolution of the occupation numbers of the neutron single-particle orbits as the residual interaction is switched with $\tau=300$ fm/c. All the curves display a quite satisfactory convergence. As we turn on correlations adiabatically, a stable correlated ground state is obtained. The deeply bound $1s_{1/2}$ and $1p_{3/2}$ neutron and proton states keep more than 95% of the single-particle occupation. Correlations have the largest effect near the Fermi surface, where they deplete the $1p_{1/2}$ states by about 10% and allow for a 6–7% population of the $1d_{3/2}$ states.

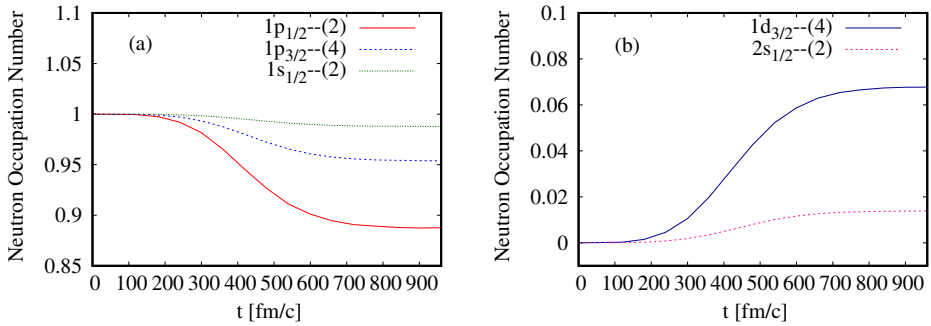

Fig. 1. Occupation numbers for the neutron orbits in ^{16}O as we adiabatically switch on the residual interaction from HF state. Panel (a) hole states, that are fully occupied in the initial HF state. Panel (b) the corresponding particle states. States and their degeneracies are labeled.

3.2. Dissipation process on macroscopic level

We consider a head-on symmetric collision, $^{16}\mathrm{O}+^{16}\mathrm{O}\rightarrow{}^{32}\mathrm{S}$, using the adiabatically evolved correlated states as projectile and target. The collective coordinate R at time t is defined as the relative distance between the center of masses, $R(t)=\langle\Psi(t)_{\rm pro}|z|\Psi(t)_{\rm pro}\rangle-\langle\Psi(t)_{\rm tar}|z|\Psi(t)_{\rm tar}\rangle$. The collective momentum P is calculated analogously.

Figure 2 shows the trajectories of both R and P. TDHF (dashed) and TDDM$^{\rm P}$ (solid line) results at an incident energy of 40 MeV are presented. In panel (a), the distance R is plotted as a function of time, whereas panel (b) shows P as a function of R. The touching point corresponds to $t\approx 50$ fm/c and $R\approx 6$ fm. Beyond this point, the TDHF and TDDM$^{\rm P}$ trajectories deviate from each other. The momentum for TDDM$^{\rm P}$ slows down faster

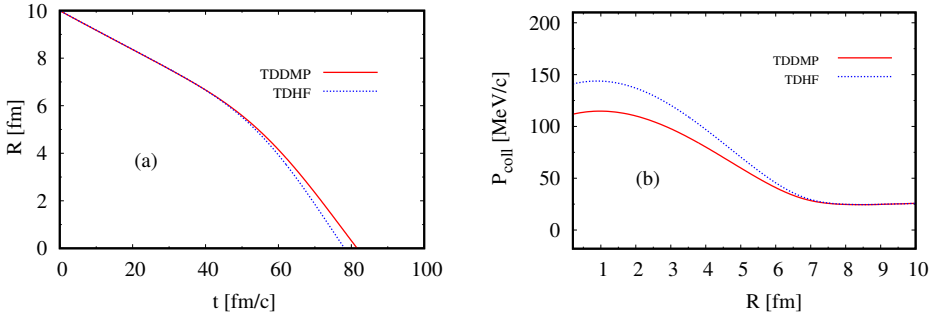

Fig. 2. (Colour on-line) (a) Relative distance R as a function of time. (b) Collective momentum P as a function of R. Both for the reaction $^{16}\mathrm{O}+^{16}\mathrm{O}\rightarrow^{32}\mathrm{S}$ at incident energy of 40 MeV. The solid (red) line shows the result of TDDM^P, while the dotted (blue) line gives the result of TDHF.

than for TDHF so that at $R = 2$ fm, the collective momentum of TDHF is larger by a third. This is a strong indication that the collective motion is more dissipative in the presence of two-body correlations.

Next, we directly compare the dissipated energy and the friction parameter of both methods. The intrinsic energy E_{intr} is obtained by subtracting the collective energy, $E_{\mathrm{coll}}(R) = T_{\mathrm{coll}}(R)+V_{\mathrm{coll}}(R)$, from the initial bombarding energy. It is worth mentioning that the one-body dissipation extracted from TDHF for low-energy fusion reactions is in a reasonable agreement with those calculated based on the linear response theory [15]. The friction coefficient $\gamma(R)$ is extracted as $\gamma(R) = \frac{\mathrm{d}E_{\mathrm{intr}}(R)}{\mathrm{d}R} \times \frac{1}{P}$. Panel (a) of Fig. 3 shows the intrinsic energy as a function of R for both methods. After contact, the intrinsic energy grows monotonically in the region $R < 6$ fm. We take the difference between TDDM^P and TDHF intrinsic energies as a further

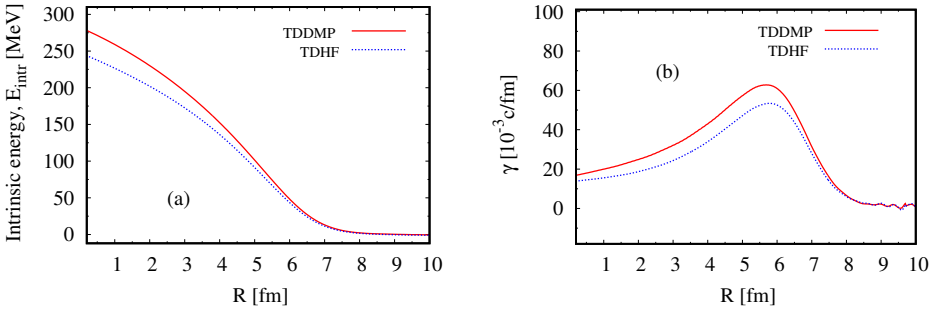

Fig. 3. (Colour on-line) Intrinsic energies (a) and friction coefficients (b) as a function of R for the reaction $^{16}\mathrm{O}+^{16}\mathrm{O}\rightarrow^{32}\mathrm{S}$ at incident energy of 40 MeV. The solid (red) line shows the result of TDDM^P, while the dotted (blue) line gives the result of TDHF.

indication of dissipation stemming from two-body correlations. Panel (b) shows the friction coefficient γ. The shapes of the friction coefficients as a function of R are very similar for the two methods. As R decreases, the friction coefficients develop a hump, and then subsequently decrease. We find that two-body correlations contribute to enhance the friction coefficient.

4. Summary

We investigated dissipative fusion dynamics with both the TDHF and TDDM^P models. We focus on the energetics of the nuclear fusion reaction $^{16}\mathrm{O} + ^{16}\mathrm{O} \rightarrow ^{32}\mathrm{S}$, and also extract the corresponding friction coefficients. Dissipation, both in terms of energy balance and friction coefficients, is enhanced noticeably by two-body correlations. We note that the form of the interaction is critical in these simulations. A more realistic future analysis should start from an effective force adjusted to the static nuclear observables within the TDDM scheme.

REFERENCES

[1] P. Bonche, S. Koonin, J. W. Negele, *Phys. Rev. C* **13**, 1226 (1976).

[2] J.A. Maruhn, P.-G. Reinhard, P.D. Stevenson, A.S. Umar, *Comput. Phys. Commun.* **185**, 2195 (2014).

[3] A. Bulgac, *Annu. Rev. Nucl. Part. Sci.* **63**, 97 (2013).

[4] T. Nakatsukasa *et al.*, *Rev. Mod. Phys.* **88**, 045004 (2016).

[5] C. Simenel, A.S. Umar, *Prog. Part. Nucl. Phys.* **103**, 19 (2018).

[6] H. Born, H. Green, *Proc. R. Soc. Lond. Ser. A* **188**, 10 (1946); N.N. Bogoliubov, *J. Phys. USSR* **10**, 265 (1946); J.G. Kirkwood, *J. Chem. Phys.* **14**, 180 (1946).

[7] M. Gong, "Time-Dependent Density Matrix Theory", Ph.D. Thesis, Michigan State University, 1990.

[8] W. Shun-Jin, W. Cassing, *Ann. Phys.* **159**, 328 (1985).

[9] M. Tohyama, *Phys. Rev. C* **36**, 187 (1987).

[10] M. Tohyama, A.S. Umar, *Phys. Lett. B* **549**, 72 (2002).

[11] M. Assié, D. Lacroix, *Phys. Rev. Lett.* **102**, 202501 (2009).

[12] K. Wen, M.C. Barton, A. Rios, P.D. Stevenson, *Phys. Rev. C* **98**, 014603 (2018).

[13] A. Rios, B. Barker, M. Buchler, P. Danielewicz, *Ann. Phys.* **326**, 1274 (2011).

[14] M. Beiner, H. Flocard, N. Van Giai, P. Quentin, *Nucl. Phys. A* **238**, 29 (1975).

[15] K. Washiyama, D. Lacroix, S. Ayik, *Phys. Rev. C* **79**, 024609 (2009).